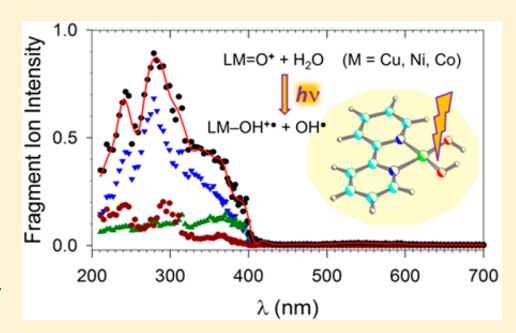
Near-UV Water Splitting by Cu, Ni, and Co Complexes in the Gas **Phase**

Andy Dang,[†] Christopher J. Shaffer,[†] Daniel Bím,[‡] John Lawler,[§] Michael Lesslie,[§] Victor Ryzhov,[§] and František Tureček*,†

Supporting Information

ABSTRACT: (2,2'-Bipyridine)M=O $^+$ ions (M = Cu, Ni, Co) were generated by collision-induced dissociation and near-UV photodissociation of readily available [(2,2'-bipyridine)M^{II}(NO₃)]⁺ ions in the gas phase, and their structure was confirmed by ion-molecule reactions combined with isotope labeling. Upon storage in a quadrupole ion trap, the (2,2'bipyridine)M=O⁺ ions spontaneously added water, and the formed [(2,2'bipyridine)M= $O + H_2O$ ⁺ complexes eliminated OH upon further near-UV photodissociation. This reaction sequence can be accomplished at a single laser wavelength in the range of 260-340 nm to achieve stoichiometric homolytic cleavage of gaseous water. Structures, spin states, and electronic excitations of the metal complexes were characterized by ion-molecule reactions using ²H



and ¹⁸O labeling, photodissociation action spectroscopy, and density functional theory calculations.

■ INTRODUCTION

Water is an extremely stable molecule, as illustrated by its molar enthalpy of formation from O_2 and H_2 (-242 kJ mol⁻¹) and its large O-H bond dissociation energy (499 kJ mol⁻¹). Perhaps for this reason, homolytic splitting of O-H bonds in water has not been pursued as a potential source of H2 and O2 for chemical energy storage. Water splitting by oxidation to O2 and H₃O⁺ is achieved by plants in a multistep four-electron process accomplished by the multienzyme photosystem II.² Artificial water oxidation has been the target of numerous studies that relied on heterogeneous and homogeneous transition metal (M) catalysts such as complexes of Mn and Ru.³⁻⁵ The mechanistic interpretation of the redox cycles presumes the existence of ligated M=O complexes that oxidize water, forming hydroperoxy intermediates.^{6,7} However, these highly reactive M=O intermediates are difficult to characterize in the condensed phase.

The rarefied gas phase is an inert medium that has been used for the generation of numerous highly reactive species in different electronic states that have been characterized by mass spectrometry.⁸ Ligated metal-oxide cations, (phen)Cu=O⁺ (phen = 1,10-phenanthroline) were first generated in the gas phase by Schröder, Schwarz, and co-workers⁹ using collisioninduced dissociation (CID) of ternary [(phen)Cu^{II}(NO₃)]⁺● ions formed by electrospray ionization. The (phen)Cu=O+ and related ions have been used to study hydrogen abstraction from C-H bonds of various gaseous molecules. 11-13 The formation of (phen)Cu=O+ was accomplished under the relatively high-pressure conditions of an electrospray ion source

and without mass-selecting the precursor ternary nitrate complex. This led to a partial isomerization of the (phen)-Cu=O+ ions to isomeric (phen-OH)Cu+ ions that were distinguished by Schwarz et al. using ion mobility, 12 and by Roithova et al. using infrared multiphoton dissociation spectroscopy measurements. 11 Isomerization of (phen)Cu= O+ to (phen-OH)Cu+ has been shown by density functional calculation to be highly exothermic. 11 These studies established that the formation of (phen)Cu=O+ and its isomerization in the gas phase depended on the experimental conditions of the applied cone voltage. 11,12 Interest in Cu complexes has been further stimulated by a recent report 14 by Mayer, Goldberg, and co-workers who described a soluble copper complex containing 2,2'-bipyridine (bpy) as a ligand that was an efficient homogeneous catalyst for electrolytic water oxidation.

We now report that simple bpy complexes of Cu, Ni, and Co in the gas phase can be used to achieve nonelectrolytic water splitting. We generated the (bpy)Cu=O⁺, (bpy)Ni=O⁺, and (bpy)Co=O+ complexes from mass-selected ion precursors and characterized them by ion-molecule reactions, ²H and ¹⁸O isotope labeling, UV-vis photodissociation action spectroscopy, and time-dependent DFT calculations. In particular, we wish to show that in situ made water adducts of the Cu, Ni, and Co complexes undergo near-UV photodissociation achieving

December 18, 2017 Received: Revised: February 8, 2018 Published: February 9, 2018

Department of Chemistry, University of Washington, Seattle, Washington 98195-1700, United States

[‡]Institute of Organic Chemistry and Biochemistry, Czech Academy of Sciences, 117 20 Prague 1, Czech Republic

[§]Department of Chemistry, Northern Illinois University, DeKalb, Illinois 60115-2828, United States

stoichiometric water splitting in the gas phase under mild conditions.

EXPERIMENTAL SECTION

Materials. Sodium nitrite, 2,2'-bipyridine, copper(II) perchlorate hexahydrate, copper(II) nitrate (97% purity or better), and all solvents were purchased from Sigma-Aldrich (Milwaukee, WI) Water-¹⁸O (normalized at 97-98 atom %) was purchased from Icon Isotopes (Summit, NJ). All purchased materials were used as received without further purification. The preparation of the [(bpy)Cu^{II}(NO₂¹⁸O)]⁺ complex is described in the Supporting Information. 6-Hydroxy-2,2'bipyridine was prepared by Pd(Ph₃P)₄-catalyzed coupling of pyridine-2-magnesium bromide with 2-bromo-6-methoxypyridine (Sigma-Aldrich) followed by hydrolysis. 15 The product was characterized by high-resolution mass spectrometry (measured m/z 173.0705, $C_{10}H_9N_2O^+$ requires 173.0709, error < 2.5 ppm) and a CID mass spectrum: m/z 173.0705, $(M+H)^+$, m/z 155 (loss of H₂O), m/z 146 (loss of HCN), m/z145 (loss of CO), m/z 131 (loss of NCO).

Mass Spectrometry. Mass spectrometry measurements were performed on a modified LTQ-XL-ETD linear ion trap (LIT) tandem mass spectrometer (ThermoElectron Fisher, San Jose, CA, USA). $[(bpy)M^{II}(NO_3)]^+$ ions were generated by electrospray ionization of methanol-water solutions containing 2,2'-bipyridine and metal (Cu, Ni, or Co)^{II} nitrates. The ions were selected by mass for the major isotopes (63Cu, 58Ni, 59Co) and stored in the ion trap at 3 mTorr of the He bath gas. CID was performed by resonant ion excitation at normalized collision energies of 10-25 system units. Photodissociation was performed using the previously described equipment. 16,1 The irradiating light beam was produced by an Nd:YAG EKSPLA NL301G laser (Altos Photonics, Bozeman, MT, USA) operating at 20 Hz frequency with a 3-6 ns pulse width. Photons exiting the pump laser are fed into a PG142C unit (Altos Photonics, Bozeman, MT, USA, which integrates a third harmonic generator and optical parametric oscillator coupled with an optional second harmonic generator (SH) to provide wavelength tuning between 210 and 409 nm at a pulse peak power ranging between 0.79 and 2.06 mJ. These powers are measured at each wavelength using an EnergyMax-USB J-10MB energy sensor (Coherent Inc., Santa Clara, CA, USA) to calibrate the spectra. The laser beam is aligned by mirrors and focused by a telescopic lens to pass the small aperture drilled in the auxiliary chemical ionization source used to produce electron donor reagent ions. The laser beam diameter in the LIT is estimated at 3-4 mm to ensure overlap with the trapped ions. Typically, 100 scans were accumulated at each wavelength, and the photofragment ion intensities were normalized to the sum of all fragment ions.

Another set of measurements with regular and ^{18}O -labeled ions were performed on a Thermo Orbitrap Velos instrument. Ions were generated by electrospray ionization, stored in the LIT at bath gas pressure and analyzed by resonant ejection from the LIT or transferred to the Orbitrap analyzer for Fourier transform mass measurements at 100,000 resolving power (fwhm). The m/z measured in the ^{18}O labeling experiments were as follows: $[(bpy)^{65}\text{Cu}^{II}(NO_2^{18}\text{O})]^+$: measured 284.9915, theoretical 284.9886; $[(bpy)^{65}\text{Cu}^{I8}]^+$: measured 238.9973, theoretical 238.9957.

Ion-molecule reactions with $\rm H_2^{18}O$ were performed on a modified Bruker Esquire 3000 ion trap tandem mass spectrometer (Bruker Daltonics, Billerica, MA, USA). The

working pressure in the ion trap was estimated at 1 mTorr He and several mTorr of water vapor introduced by a leak valve.

Calculations. Standard ab initio and density functional theory calculations were performed with the Gaussian 09 suite of programs. 19 All structures were obtained by gradient optimization using the B3LYP²⁰ CAM-B3LYP,²¹ ω B97X-D,²² and M06²³ hybrid functionals with the 6-311+G(2d,p) basis set and confirmed as local energy minima by harmonic frequency calculations, which gave all real frequencies. The optimized structures are available from the corresponding author upon request. All calculations of open-shell species were performed within the spin-unrestricted formalism. Vertical excitation energies were obtained by time-dependent DFT calculations²⁴ using the M06 functional and the 6-311++G(3df,2p) basis set in a spin unrestricted formalism. The choice of the M06 functional was based on benchmarking against the experimental absorption and UVPD action spectra of [(bpy)M(NO₃)]⁺● complexes (M = Cu, Ni, Co), where M06 TD-DFT calculations showed the best match, as discussed later in the paper. Typically 30-40 excited states were generated by TD-DFT calculations. Vibronic absorption spectra were calculated for 30 excited states from 500 configurations generated at 300 K by the Newton-X program.²⁵

RESULTS AND DISCUSSION

Formation of (bpy)M=O⁺ lons. The reactive complexes, (bpy)M=O⁺, where M = Cu, Ni, and Co, were generated from ternary transition metal nitrate complexes obtained by electrospray ionization of aqueous-methanol solutions. ²⁶ To illustrate this with the Cu ions, $[(bpy)Cu(NO_3)]^{+\bullet}$ ions were formed by electrospray, selected by mass (m/z 281 for the ⁶³Cu isotope), and stored in the ion trap. The ions were subjected to CID, resulting in elimination of NO₂ (Figure 1a) thus forming (bpy)Cu=O⁺ ions ⁹ that were selected by mass (m/z 235) and stored in the ion trap. Analogously, laser photodissociation ¹⁶ of gas-phase $[(bpy)Cu(NO_3)]^{+\bullet}$ resulted in elimination of NO₂ and formation of $(bpy)Cu=O^+$ (Figure 1b). The $(bpy)Co=O^+$ and $(bpy)Ni=O^+$ ions were generated analogously from

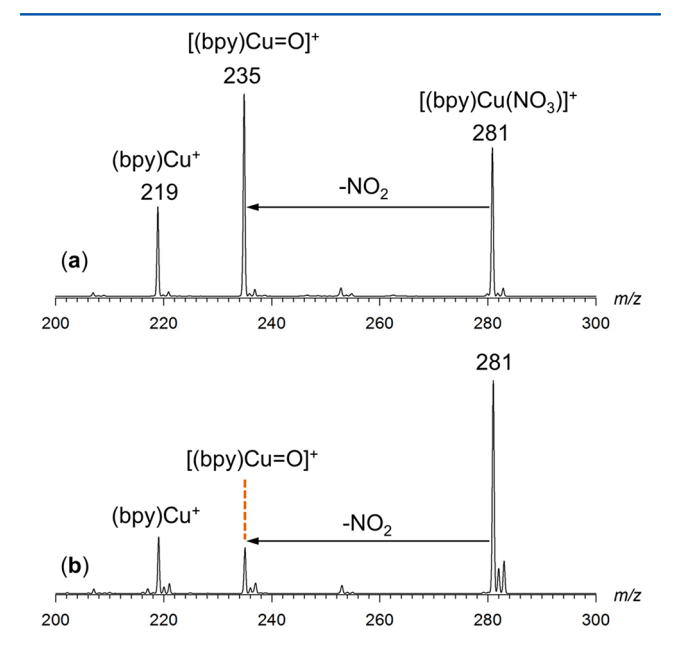


Figure 1. (a) Collision-induced dissociation and (b) 299 nm single-pulse photodissociation spectra of $[(bpy)^{63}Cu(NO_3)]^{+\bullet}$ complexes.

the respective nitrate complexes (Figure S1a—d, Supporting Information). An alternative method of generating (bpy)Cu=O⁺ ions by CID of a mass-selected perchlorate complex, [(bpy)Cu(ClO₄)]^{+•}, m/z 318 for the ³⁵Cl and ⁶³Cu isotopes, was less efficient, chiefly leading to loss of ClO₄ and forming the Cu(bpy)⁺ fragment ions (Figure S2a,b, Supporting Information). This result differs from those reported by Roithova et al., who used perchlorate complexes for the formation of LCuO⁺ ions with various ligands (L) under high pressure conditions of an electrospray interface. ¹³ All Cucontaining ions we generated in the linear ion trap were characterized by appropriate accurate mass measurements shown in Table S1 (Supporting Information).

The (bpy)M=O⁺ ions underwent a facile reaction with residual water vapor upon storage in the ion trap, forming [(bpy)M=O + H₂O]⁺ adducts as the only products. The water addition showed a pseudo-first order rate of depletion of the reactant ions (Figure S3a-c, Supporting Information). The absolute rate constants were not determined because the water vapor pressure could not be measured accurately; kinetic measurements that were performed on different types of ion trap instruments showed different reaction rates. The relative rates were simultaneously measured for the Cu-Co and Cu-Ni pairs of complexes whose isotopes are well mass-resolved. Figure 2 shows the semilog plots of the (bpy)M=O⁺ ion molar

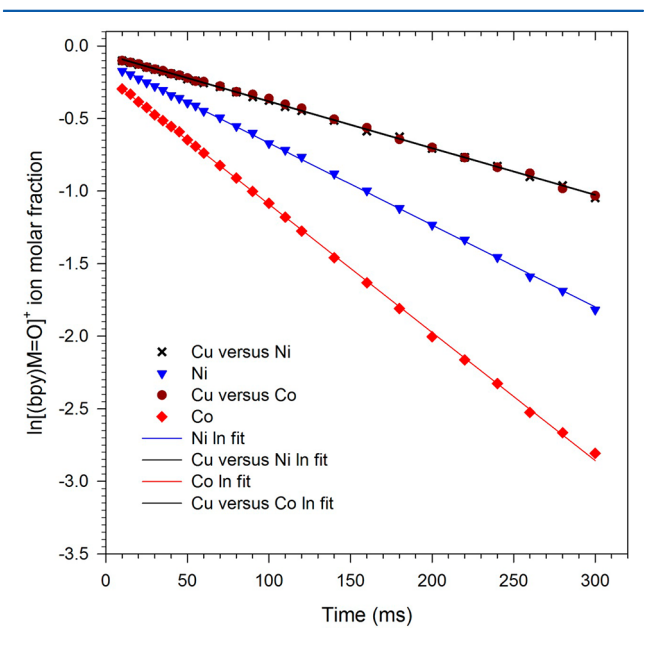


Figure 2. Logarithmic plots for reactions of (bpy)Cu=O⁺, (bpy)Ni=O⁺, and (bpy)Co=O⁺ with water.

fractions. The curves for (bpy)Cu=O⁺ ion depletion via reaction with background water when plotted against those for Ni and Co complexes are perfectly overlapping, indicating identical conditions for all three metal complexes. From these measurements, the (bpy)Co=O⁺ ion showed the largest relative rate constant for water addition ($k' = 8.8 \text{ s}^{-1}$, $r^2 = 0.9996$), followed by (bpy)Ni-O⁺ ($k' = 5.6 \text{ s}^{-1}$, $r^2 = 0.9996$), whereas (bpy)Cu=O⁺ was the least reactive ($k' = 3.2 \text{ s}^{-1}$, $r^2 = 0.9996$). The different rates are also reflected by the kinetic curves (Figure S3, Supporting Information) that show increasing fractions of (bpy)M=O⁺ ions, 0.06, 0.10, and 0.19, for Cu, Ni, and Co, respectively, which were already

depleted at t=0 during the preceding 20 ms precursor ion isolation time window.

Structure Characterization of $[(bpy)M=0 + H_2O]^+$ **lons.** Previous reports indicated that (phen)Cu=O⁺ ions can undergo internal oxygen transfer to the phenanthroline ligand forming a 2-hydroxyphenanthroline isomer, (2-OH-phen)-Cu⁺. In light of those results, we probed the structural integrity of the bpy ligand in the (bpy)M=O+ ions formed in the ion trap. To this end we utilized the facile addition of water to elucidate the structure of the closely related [(bpy)M=O +H₂O]⁺ adducts using two different probes. In the first probe aimed at the bpy ligand, we generated (D₈-bpy)M=O⁺ ions by CID of $[(D_8\text{-bpy})M(NO_3)]^{+\bullet}$ complexes, as shown in Figure S4a-c (Supporting Information). The (D₈-bpy)M=O⁺ ions were isolated by mass and allowed to react with residual water forming the respective $[(D_8-bpy)M=O+H_2O]^+$ adducts. The adducts were stored in the ion trap for up to 2 s. Assuming that the D₈-bpy ligand underwent oxygen insertion forming a D₇bpy-OD in an isomeric complex, as reported for phenanthroline, 9,11 the newly formed OD group would be expected to undergo gradual D/H exchange with the added light water and surrounding water vapor. However, less than 0.1% D/H exchange was observed for all [(D₈-bpy)M=O + H₂O]⁺ complexes after having been stored in the ion trap for 2 s, indicating that the D atoms remained in the nonexchangeable positions in the bpy ligand.

Further probing by CID of $[(D_8-bpy)M=O + H_2O]^+$ complexes gave different results for Co and Ni on one hand and Cu on the other. CID of $[(D_8-bpy)Co=O + H_2O]^+$ and $[(D_8\text{-bpy})\text{Ni}=O + H_2O]^+$ ions produced the respective $(D_8\text{-}$ bpy)Co=O⁺ and (D₈-bpy)Ni=O⁺ ions that, upon storage in the ion trap, added water without D/H exchange (Figure S5, Supporting Information). These results indicated that the bpy ligand remained intact in the Co and Ni complexes even after collisional activation. By contrast, collisional activation of [(D₈bpy)Cu=O + H₂O]⁺ resulted in loss of H₂O that was accompanied by D/H exchange in a 55% fraction of the ions, giving the respective D_8 and D_7 $[(D_x-bpy)Cu=O + H_2O]^+$ ions after spontaneous water readdition (Figure 3a,b). This result is consistent with previous studies of (phen)Cu=O+ ions, where isomerization by oxygen transfer to the ligand was promoted by collisional activation. 11,12

An additional probe was based on comparing the properties of (bpy)Cu=O⁺ and $[(bpy)Cu=O + H_2O]^+$ ions with those of authentic (6-OH-bpy)Cu⁺ and $[(6\text{-OH-bpy})Cu + H_2O]^+$

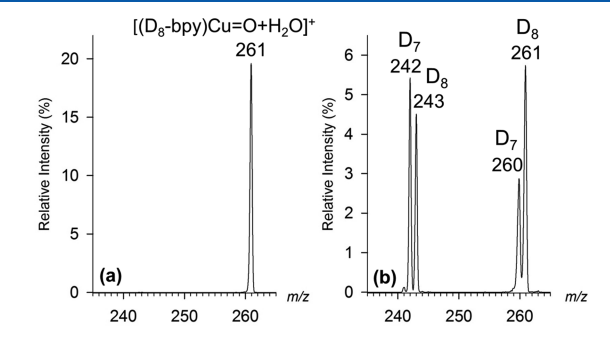
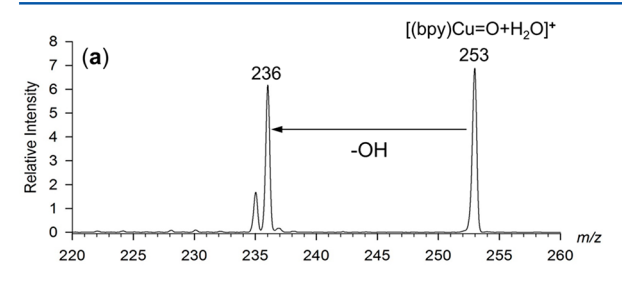


Figure 3. Mass spectra of $[(D_8\text{-bpy})Cu=O + H_2O]^+$ ions $(m/z\ 261)$ formed by CID (100 ms) of $[(D_8\text{-bpy})^{63}Cu(NO_3)]^{+●}$ followed by water addition. (a) H/D exchange by ion—molecule reactions for 2000 ms with no additional excitation. (b) H/D exchange for 300 ms with CID excitation (100 ms).

isomers. The latter ions were generated by CID of the $[(6\text{-}OH-bpy)Cu^{II}(CH_3COO)]^+$ complex (m/z 294 for the ^{63}Cu isotope) prepared by electrospray of an aqueous-methanol solution of 6-hydroxy-2,2'-bipyridine, $CuSO_4$ and acetic acid. CID of the $[(6\text{-}OH-bpy)Cu(CH_3COO)]^+$ ion (Figure S6a, Supporting Information) produced the $(6\text{-}OH-bpy)Cu^+$ ions at m/z 235 that spontaneously added water upon storage in the ion trap, forming $[(6\text{-}OH-bpy)Cu + H_2O]^+$ at m/z 253 (Figure S6b). The water addition was reversible, as documented by CID of the water adduct that reformed $(6\text{-}OH-bpy)Cu^+$ (Figure S6c). The $[(6\text{-}OH-bpy)Cu + H_2O]^+$ ions were further probed by UVPD at 311 nm (Figure 4). Whereas UVPD of



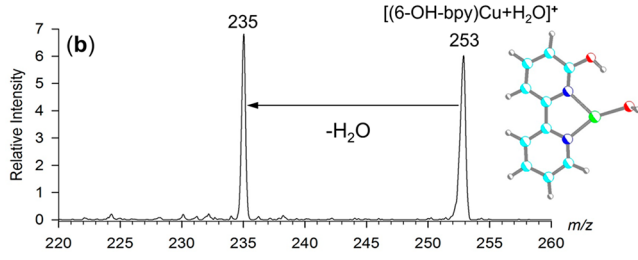


Figure 4. Photodissociation spectra (311 nm, single 12 mJ laser pulse) of (a) $[(bpy)^{63}Cu=O+H_2O]^+$ and (b) $[(6\text{-}OH\text{-}bpy)^{63}Cu+H_2O]^+$.

[(bpy)Cu=O + H_2O]⁺ resulted in a dominant loss of OH (Figure 4a), UVPD of [(6-OH-bpy)Cu + H_2O]⁺ ions resulted in an exclusive loss of the water ligand (Figure 4b). In summary, these combined D/H exchange and UVPD experiments provided strong evidence for the structure integrity of the [(bpy)Cu=O + H_2O]⁺ ions and their (bpy)Cu=O⁺ precursors, and further highlighted the unique reactivity of the ligated M=O⁺ complexes.

Oxygenated Ligands in $[(bpy)M=O + H_2O]^+$ Ions. Ligation of the two oxygen and hydrogen atoms in the $[(bpy)M=O + H_2O]^+$ complexes raised further questions about the nature of the oxygenated ligands. The possible combinations, a H2O2 molecule, two hydroxyl groups ligated to the metal ion, or a water adduct to a metal-oxo complex, were distinguished by using specific ¹⁸O labeling of the oxygen atoms introduced sequentially into the metal complexes. In these experiments, we probed ligand exchange combined with complementary ¹⁸O isotope labeling. An ion-molecule reaction of the (bpy)⁶⁵Cu=O⁺ (m/z 237) ion with H₂¹⁸O that was introduced into the ion trap 18,27 produced the [(bpy)Cu=O + $H_2^{18}O$] adduct that was isolated by mass (m/z 257). The ⁶⁵Cu isotope was selected to avoid overlap of 63Cu18O and 65Cu16O isobars due to spurious light water in the ion trap. Resonant excitation and CID of [(bpy)⁶⁵Cu=O + H₂¹⁸O]⁺ produced exclusively (>99%) (bpy) 65 Cu=O⁺ (m/z 237, Figure 5a) by elimination of H₂¹⁸O. Hence, under these conditions, the oxygen atoms in the water adduct were nonequivalent and did not undergo equilibration by proton transfer. The reversible

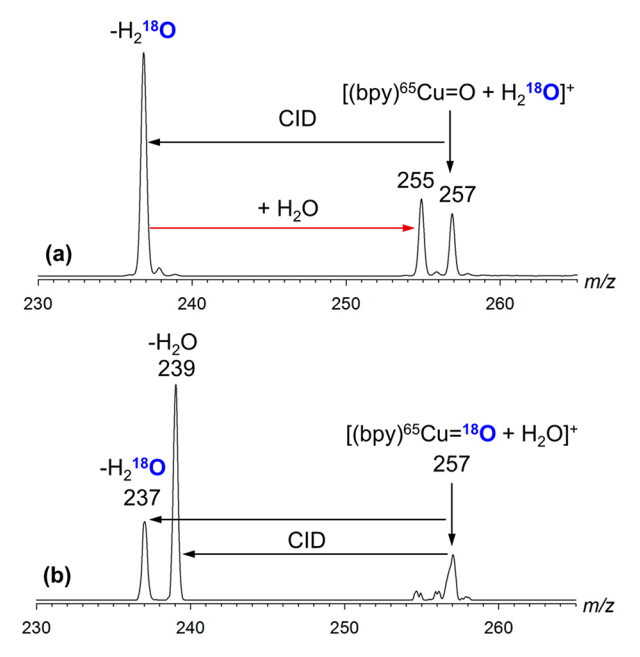


Figure 5. Collision-induced dissociation mass spectra of (a) $[(bpy)^{65}Cu=^{18}O + H_2O]^+$ and (b) $[(bpy)^{65}Cu=O + H_2^{18}O]^+$ ions.

nature of the water elimination-addition is apparent from the CID spectrum of $[(bpy)^{65}Cu=O + H_2^{18}O]^+$ (Figure 5a) that shows the formation of $[(bpy)^{65}Cu=O + H_2O]^+$ at m/z 255 by reaction with background light water during the CID excitation time.

Contrasting results were obtained for the complementary reaction with light water of the ¹⁸O labeled Cu complex, $(bpy)^{65}Cu=^{18}O^{+}$ at m/z 239, that was generated by CID of [(bpy)⁶⁵Cu^{II}(NO₂¹⁸O)]⁺ in another ion trap mass spectrometer operating under lower water pressure conditions (Orbitrap Velos) and characterized by accurate mass measurements, as described in the Supporting Information. Addition of light water followed by resonant excitation CID of mass-selected $[(bpy)^{65}Cu=^{18}O + H_2O]^+$ gave two products by loss of H_2O and H₂¹⁸O in a 71:29 ratio (±0.08) as an average of measurements at three collision energies (Figure 5b). This indicated oxygen equilibration by hydrogen migration in a 0.58 molar fraction of the water adduct complex, whereas a 0.42 molar fraction corresponded to unscrambled [(bpy)⁶⁵Cu=¹⁸O $+ H_2O$]⁺. We interpret these results as being due to a different composition of water adducts to (bpy)Cu=O+ ions generated under different conditions. Water adducts generated at a higher background water pressure contained nonequivalent oxygenated ligands, whereas water addition at a low pressure formed a mixture of complexes containing both types of ligands.

Addition of $H_2^{18}O$ to the (bpy)Ni=O⁺ and (bpy)Co=O⁺ ions formed adducts that were selected by mass $(m/z\ 250\ and\ 251$, respectively) and investigated by CID. The [(bpy)Ni=O⁺ + $H_2^{18}O$]⁺ ion competitively eliminated $H_2^{18}O$ and light water in a 4:3 ratio, indicating prevalent equilibration of the ligated oxygen atoms (Figure S7a, Supporting Information). The data analysis was complicated by the rapid reverse addition of light and heavy water to the (bpy)Ni=O⁺ product ions that formed adducts $(m/z\ 248,\ 250,\ and\ 252)$ in which the oxygen atoms were scrambled. The [(bpy)Co=O⁺ + $H_2^{18}O$]⁺ ion also competitively eliminated $H_2^{18}O$ and light water, but because of

the very fast reverse water addition, the label scrambling was extensive (Figure S7b).

UV Water Splitting and Action Spectra. Photodissociation at 311 nm of the $[(bpy)Cu=O + H_2O]^+$ complex revealed that near-UV electronic excitation resulted in the splitting of the ligated water molecule and release of an OH radical. Considering the overall sequence for the gas-phase reactions involving $(bpy)Cu=O^+$ (eq 1), near-UV photodissociation effectively achieved dissociation of the water molecule

$$[(bpy)Cu=O]^{+} + H_{2}O \rightarrow [(bpy)Cu=O + H_{2}O] +$$

$$\rightarrow (bpy)Cu-OH^{+\bullet} + OH^{\bullet}$$
(1)

that was mediated by the Cu complex. This contrasts direct photodissociation of gaseous water that requires wavelengths in the vacuum UV region (<180 nm).²⁸ This unexpected result prompted us to investigate UVPD of the [(bpy)M=O + H₂O]⁺ and related ion complexes over a broader range of wavelengths. To begin with, we obtained a UV-vis photodissociation action spectrum¹⁷ of mass-selected [(bpy)-CuNO₃]^{+•} (Figure S8a, Supporting Information). The spectrum was similar to the absorption spectrum of (bpy)Cu-(NO₃)₂ measured in aqueous-methanol solution (Figure S8b), indicating that the gas-phase structure and electronic properties of this ion were similar to those of the species in solution. The photodissociative elimination of NO₂ (fragment ion m/z 235) showed broad maxima at 285 and 240 nm and competed with a minor loss of NO_3^{\bullet} (fragment ion at m/z 219, Figure S8a). The electronic transitions pertinent to the photodissociation are shown in the TD-DFT calculated absorption spectrum (Figure S8c).

Near-UV photodissociation of the Ni^{II} and Co^{II} bpy complexes gave similar results. The action spectrum of [(bpy)NiNO₃]^{+•} (⁵⁸Ni, *m/z* 276) showed well-developed absorption maxima at 290 and 310 nm, extending by a weaker arm to 350 nm. Further broad bands appeared at 230–250 nm (Figure S9a, Supporting Information). The [(bpy)CoNO₃]^{+•} (⁵⁹Co, *m/z* 277) complex showed a band centered at 306 nm and a weaker broad band stretching from 280 to 210 nm (Figure S9b). In both cases, the main photodissociation channel corresponded to loss of NO₂, forming the respective (bpy)Ni=O⁺ and (bpy)Co=O⁺ ions.

Photodissociation of the water adducts was investigated by UV-vis action spectroscopy (Figure 6a,b). The [(bpy)Cu=O + H₂O]⁺ complex showed three dissociation channels; a major loss of OH (m/z 236), and less abundant loss of H₂O (m/z235), and 2OH (m/z 219) (Figure 6a). The loss of OH showed absorption maxima at 330 (broad), 315, 280, and 244 nm. The loss of water displayed a broad band with a maximum at 370 nm and less pronounced ones at 315 and 245 nm. The m/z 219 dissociation channel showed maxima at 365, 296, and 244 nm. No photodissociation was observed near 617 nm (Figure S10, Supporting Information) where the [(bpy)Cu(OH)₂]⁺ complex was reported to absorb in aqueous solution.²⁹ The UVPD action spectrum of the isomeric [(6-OH-bpy)Cu + H₂O]⁺ complex (Figure 6b) showed a major band with a maximum at 305 nm that was almost entirely due to the m/z 235 (loss of water) channel. Loss of OH became significant at short wavelengths of <230 nm. The data in Figure 6a and 6b show that the UVPD action spectra of the isomeric complexes were distinctly different. In particular, the m/z 235 loss of water showed a very minor shoulder in the spectrum of the

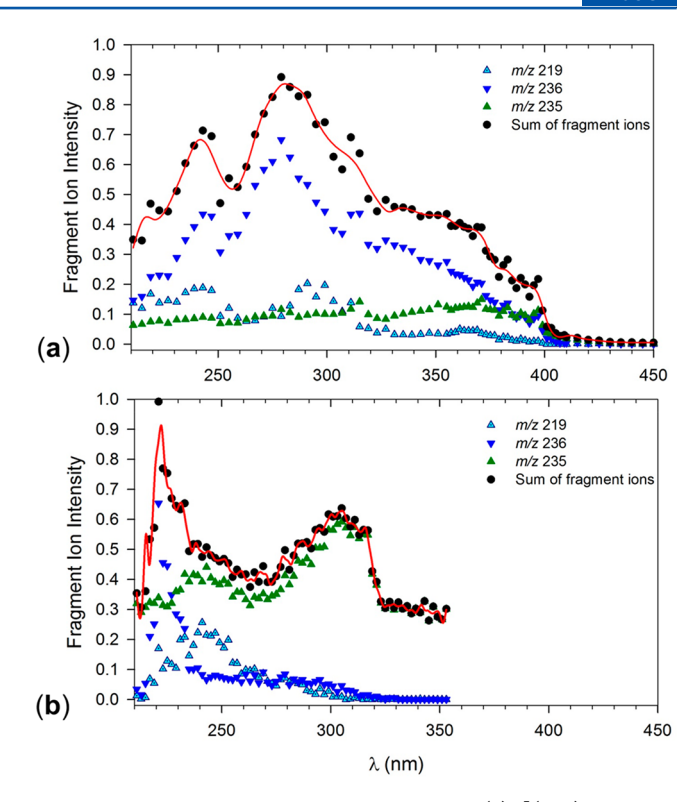


Figure 6. Photodissociation action spectra of (a) $[(bpy)Cu=O + H_2O]^+$, (b) $[(6\text{-}OH\text{-}bpy)Cu + H_2O]^{+\bullet}$. Blue triangles: loss of OH channel; green triangles: loss of water channel; black circles: sum of photofragment ion intensities.

[(bpy)Cu=O + H_2O]⁺ complex (Figure 6a). We note that this complex undergoes loss of water upon collisional activation, which proceeds from vibrationally excited ground electronic state of the ion. The minor fraction of water loss upon photodissociation can be assigned to ions that underwent internal conversion from the excited electronic state to the vibrationally excited ground state. It should be noted that, whereas collisional activation of [$LCu=O + H_2O$]⁺ complexes with dicoordinating auxiliary ligands results in loss of water, CID of an acetonitrile complex, 13 [(CH_3CN) $Cu=O + H_2O$]⁺, has been reported to result in elimination of OH in a process analogous to the above-described photodissociation.

The $[(bpy)Ni=O + H_2O]^+$ ion showed major absorption bands at 230, 310, and 340 nm with an arm extending to 420 nm (Figure 7a). A weak absorption band was observed at 590 nm. In contrast to the Cu complex, the Ni complex showed dominant loss of water (m/z 230) that peaked at 310 and 240 nm. The 230, 310, and 340 nm bands were also observed for the $[(bpy)Co=O + H_2O]^+$ ion that further showed a well developed band with a maximum at 430 nm (Figure 7b). However, the Co complex showed a different course for the elimination of OH (m/z 232) that peaked at 230 and 310 nm, whereas loss of water was slightly more abundant at 340 and 430 nm.

Ion Electronic Structures. In order to interpret the dissociations and light absorption characteristics of the complexes we carried out extensive DFT and TD-DFT calculations. The optimized structures of the Cu, Ni, and Co complexes are shown in Figures S11, S12, and S13, respectively, of the Supporting Information. The calculated M—O bond lengths in (bpy)M=O⁺ were substantially shorter than in the covalent water adducts, justifying the formulas with M=O

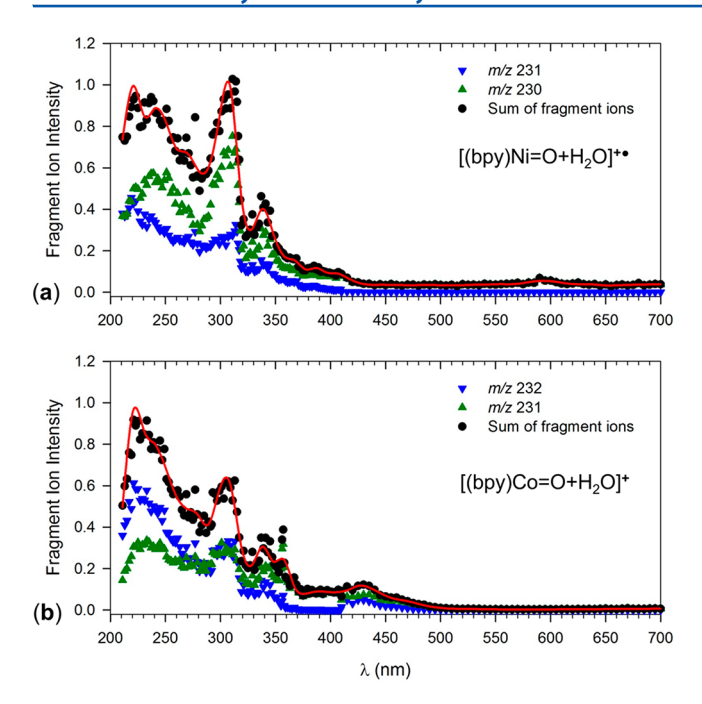


Figure 7. Photodissociation action spectra of (a) $[(bpy)Ni=O + H_2O]^{+\bullet}$, (b) $[(bpy)Co=O + H_2O]^{+}$ complexes. Blue triangles: loss of OH channel; green triangles: loss of water channel; black circles: total photofragment ions.

double bonds. We note that the analogous (phen)Cu=O⁺ ion structures and energetics have been analyzed previously by Schröder, Roithova et al.¹¹ Starting with the Cu complexes, the ground electronic state of the (bpy)Cu=O⁺ ion is a triplet (1, ³A₂)⁹ whereas the singlet state (2, ¹A") is substantially less stable. The singlet—triplet energy difference was 94–106 kJ

mol⁻¹ according to calculations by four DFT methods (Table 1). The ω B97X-D/6-311+G(3df,2p) data are discussed in the text and displayed in the potential energy diagram ($\Delta H^{\circ}_{g,0}$). Figure 8a). Attachment of a water molecule to 1 was continuously exothermic (Figure S14, Supporting Information) leading to a complex (3) at -32 kJ mol⁻¹ relative to the reactants. The reaction free energy was calculated as $\Delta G^{\circ}_{g,310}$ = 1.2 kJ mol⁻¹ at 310 K, indicating that this stage of the addition is reversible. Complex 3 can be further stabilized by forming a Cu–OH₂ covalent bond in a triplet intermediate 4 at -64 kJ mol⁻¹ relative to the reactants. Ion 4 can undergo a facile isomerization by proton migration between the OH₂ and O groups (E_{TS1} = 28 kJ mol⁻¹ relative to 4), exothermically forming a symmetrical adduct with equivalent Cu-ligated OH groups (5, Figure 8a).

Addition of water to the singlet ion **2** was continuously exothermic. At the Cu–OH₂ distance of 2.2 Å the water molecule rotated about the Cu–O axis over a small potential energy ridge (8–10 kJ mol⁻¹), allowing one of the protons to approach the other Cu-bound oxygen atom. This was followed by an exothermic proton transfer forming adduct **6**. The PES indicated that the singlet and triplet states can interconnect through a surface crossing³⁰ at distances of $r(\text{Cu-OH}_2) \leq 2.15$, leading to the more stable singlet adduct **6**.

The nature of the (bpy)Cu=O⁺ water adduct formed by the ion—molecule reaction was elucidated by analyzing the UVPD action spectrum of the m/z 253 ion (Figure 6a) using TD-DFT calculations (Figure 9a-c). First, the TD-DFT-calculated excitation energies were benchmarked on the action spectra of (bpy)[CuNO₃]^{+•} (Figure S8a) and (bpy)Cu⁺ (Figure S15a, Supporting Information), which showed excellent agreement for the M06/6-311+G(2d,p) and 6-311+G(3df,2p) calculations (Figure S8b and S15b, respectively) that were then used for the other species. The bands in the action spectrum of [(bpy)Cu=

Table 1. Energies of (bpy)Cu Ion Complexes

	relative energy (kJ mol $^{-1}$) a							
	B3LYP		CAM-B3LYP		ωB97X-D		M06	
ion or reaction	A^b	B ^c	A	В	A	В	A	В
Triplet Energies								
$[(bpy)CuNO_3]^{+\bullet} \rightarrow (^3A_2)1 + NO_2$	244	247	268	271	278	281	282	283
$1 + H_2O \rightarrow 3$	-28	-25	-33	-30	-35	-32	-36	-33
$1 + H_2O \rightarrow 4$	-50	-47	-66	-63	-68	-64	-71	-68
$4 \rightarrow 5$	-19	-8	-8	2	-19	-9	-9	1
$TS1(4 \rightarrow 5)$	24	24	24	24	29	28		
$4 \rightarrow (^2A'')Cu(bpy)OH^{+\bullet} + OH^{\bullet}$	77	74	88	85	91	88	102	99
$(bpy)Cu-OH^{+\bullet} \rightarrow 1 + H^{\bullet}$	451	454	458	462	457	461	454	458
$(bpy)Cu-OH^{+\bullet} \rightarrow Cu(bpy)^{+} + OH^{\bullet}$	236	239	238	241	237	240	226	228
$(bpy)Cu-OH^{+\bullet} \rightarrow Cu(bpy-H)^{+\bullet} + H_2O$	207	206	212	212	211	210	188	185
$(bpy)Cu-OH^{+\bullet} \rightarrow (^2A'')CuOH^{+\bullet} + bpy$	468	471	508	512	507	510	496	499
$(bpy)Cu-OH^{+\bullet} + OH^{\bullet} \rightarrow 1 + H_2O$	-27	-27	-22	-22	-23	-23		
Singlet Energies								
$[(bpy)CuNO_3]^{+\bullet} \rightarrow (^1A'')2 + NO_2$	339	340	374	375	384	385	375	375
$2 + H_2O \rightarrow 6$	-221	-218	-231	-230	-232	-230	-235	-233
$2 + H_2O \rightarrow 7$	-110	-107	-136	-132	-139	-136	-131	-128
$2 + H_2O \rightarrow 8$	-408	-408	-444	-444	-451	-451	-461	-461
$(bpy)Cu^+ \rightarrow Cu^+ + bpy$							403	406
$(bpy)Cu^+ \rightarrow Cu + bpy^{+\bullet}$							454	457
bpy → bpy ⁺ •							805	805
$Cu \rightarrow Cu^{+}$							754	754

^aIncluding zero-point energy corrections. ^bCalculations with the 6-311+G(2d,p) basis set. ^cCalculations with the 6-311+G(3df,2p) basis set.

The Journal of Physical Chemistry A

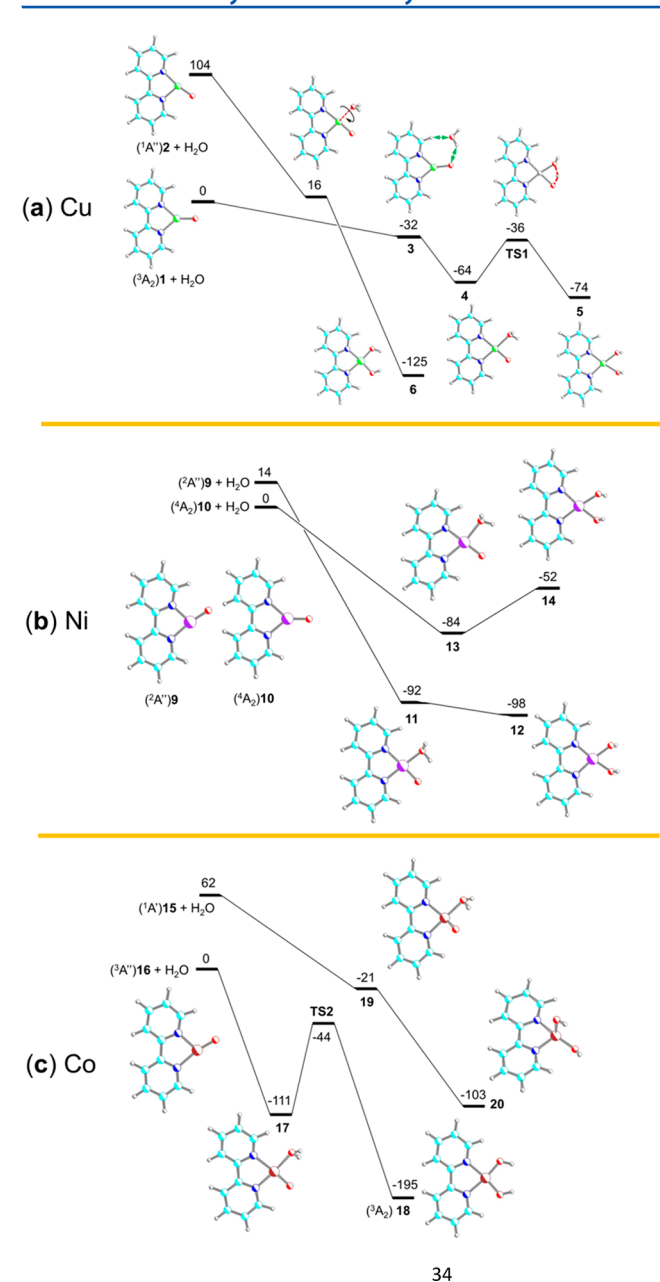


Figure 8. Potential energy diagram (kJ mol⁻¹) for (a) Cu, (b) Ni, and (c) Co complexes relative to the $[(bpy)M=O]^+ + H_2O$ reactants. From ω B97X-D/6-311+G(3df,2p) calculations including zero-point vibrational energy corrections.

O + H₂O]⁺ appear in the TD-DFT absorption spectra of 6 and 4 (Figure 9a,b), but cannot be represented by a single species. In particular, the long wavelength band in the action spectrum extending to 400 nm is prominent in the absorption spectrum of the triplet complex 4, where it appears at 325 nm ($\Delta E = 3.81$ eV) and is further broadened and red-shifted by vibronic transitions at 310 K (Figure 9b). The pertinent electron transition, MO61 $\beta \rightarrow$ MO64 β , involves Cu-centered $\sigma_{x,y}$ and $\sigma_{x,y}$ * molecular orbitals (MO) (Figure S16, top, Supporting Information). The intense band at 292 nm (Figure 9b) is assigned to the bpy π (MO64 α) $\rightarrow \pi$ *(MO66 α) transition ($\Delta E = 4.25$ eV, Figure S16, top). However, the spectrum of 4 does not display an abundant band at 240 nm, which is prominent in the action spectrum. This band appears at 237 nm ($\Delta E = 5.22$ eV) in the calculated spectrum of 6 (Figure 9a) and arises from

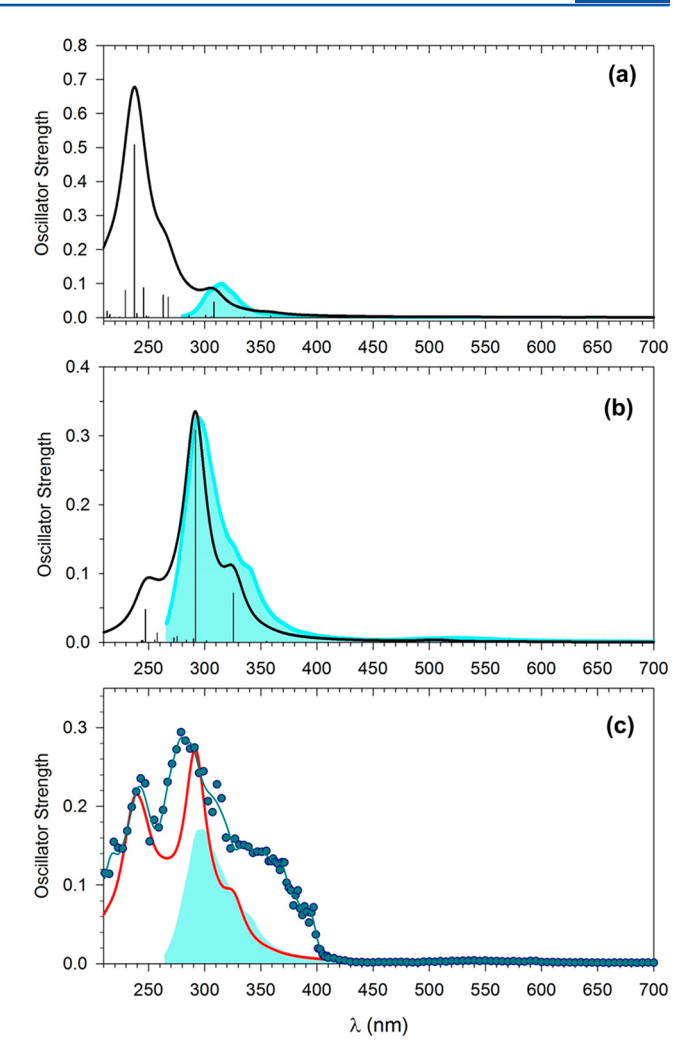


Figure 9. TD-DFT M06/6-311+G(3df,2p) calculated absorption spectra of (a) 6 and (b) 4. The green-shaded curves are from TD-DFT calculations of top 30 excited states including vibronic transitions from 500 configurations sampled at 310 K. (c) Fit of the intensity-scaled action spectrum of $[(bpy)Cu=O+H_2O]^+$ (green circles and fitting curve) and the calculated absorption spectrum of a 3:1 mixture of 4 and 6 (red curve and green shaded area).

combined $\pi_z \to \pi_z^*$ transitions within the bpy ligand and $\sigma_{x,y} \to$ $\sigma_{x,y}^*$ transitions involving the Cu-centered molecular orbitals (Figure S16, bottom). Combining the calculated spectra of of 4 and 6 in a 3:1 mixture then provides an excellent fit to the action spectrum after intensity scaling (Figure 9c). It is noteworthy that the calculated absorption spectrum of the covalent triplet adduct 5 (Figure S17a, Supporting Information) shows bands at 295 and 270 nm that can account for some minor features in the action spectrum. Thus, the presence of 5 in the adduct cannot be excluded, but it is unlikely to represent a major component. Other plausible structures, such as a $[(bpy)Cu-\mu-H_2O_2]^+$ adduct (7) and a [(6-OH-bpy)Cu-OH₂] complex (8) were examined but gave absorption spectra that were incompatible with the action spectrum, as shown in Figures S17b and S17c, respectively, of the Supporting Information. It is noteworthy that none of the gas-phase [(bpy)Cu(OH)₂]⁺ isomers showed a strong absorption band at 617 nm that has been reported in solution. 14,29 Weak bands (oscillator strength < 0.001) were calculated at 579 and 595 nm for **5** and at 651 nm for **6**.

The Journal of Physical Chemistry A

Table 2. Energies of (bpy)Ni Ion Complexes

	relative energy (kJ mol^{-1}) a						
	CAM-B3LYP		ωB97X-D		M06		
ion or reaction ^b	A ^c	B^d	A	В	A	В	
$[(bpy)NiNO_3]^+ \rightarrow (^2A'')9 + NO_2$	302		312	314	348	332	
$[(bpy)NiNO_3]^+ \rightarrow (^4A_2)10 + NO_2$	287		298	300	296	297	
$(^{4}A_{2})10 \rightarrow (^{2}A'')9$	15	13	15	14	52	35	
$9 + H_2O \rightarrow 11$	-111	-109	-110	-107	-140	-119	
$9 + H_2O \rightarrow 12$	-113	-111	-115	-112	-140	-119	
$+ H_2O \rightarrow 13$	-85	-82	-89	-84	-79	-73	
$10 + H_2O \rightarrow 14$	-56	-32	-41	-52	-10	-12	
$13 \to (^3A'')(bpy)Ni-OH^+ + OH^{\bullet}$	109	106	112	109	25	21	
$(^3A'')(bpy)Ni-OH^+ \rightarrow 10 + H^{\bullet}$	456	459	430	459	431	433	
$((^3A'')(bpy)Ni-OH^+ \rightarrow (^2B_2)Ni(bpy)^{+\bullet} + OH^{\bullet}$	289	291	289	291	169	170	
$(^{3}A'')(bpy)Ni-OH^{+} \rightarrow (^{3}A'')NiOH^{+} + bpy$	510	512	506	508	500	502	
$(^{3}A'')(bpy)Ni-OH^{+} + OH^{\bullet} \rightarrow (^{4}A_{2})10 + H_{2}O$	-24	-24	-23	-25	54	52	

^aIncluding zero-point energy corrections. ^bFor ion structures refer to Figure 7b. ^cCalculations with the 6-311+G(2d,p) basis set. ^dCalculations with the 6-311+G(2d,p) basis set.

Table 3. Energies of (bpy)Co Ion Complexes

	relative energy (kJ mol^{-1}) a						
	CAM-B3LYP		ωB97X-D		M06		
ion or reaction ^b	A ^c	B^d	A	В	A	В	
$(^{2}A_{2})[(bpy)Co(NO_{3})]^{+} \rightarrow (^{1}A')15 + NO_{2}$	329		331	330	350	347	
$(^{2}A_{2})[(bpy)Co(NO_{3})]^{+} \rightarrow (^{3}A'')16 + NO_{2}$	255		266	264	272	267	
$(^{3}A'')$ 16 \rightarrow $(^{1}A')$ 15	73		61	62	78	79	
$16 + H_2O \rightarrow (^3A)17$	-109		-116	-111	-120	-114	
$16 + H_2O \rightarrow (^3A_2)18$	-212		-218	-195	-174	-168	
17→18	-103	-103	-86	-86	-51	-50	
$TS2(17 \rightarrow 18)$	69	66	69	67			
$16 + H_2O \rightarrow (^1A)19$	-18		-27	-21	-17	-10	
$16 + H_2O \rightarrow (^1A)20$	-103		-107	-103	-98	-91	
18 → $(^{4}A)(bpy)Co-OH^{+} + OH^{\bullet}$	220	220	207	207	93	89	
$(^{4}A)(bpy)Co-OH^{+} \rightarrow 16 + H^{\bullet}$	471	517	474	474	457	457	
$(^{4}A)(bpy)Co-OH^{+} \rightarrow (^{3}B_{2})(bpy)Co^{+} + OH^{\bullet}$	443	441	442	440	246	249	
$(^{4}A)(bpy)Co-OH^{+} \rightarrow (^{4}A'')CoOH^{+} + bpy$	497	537	495	496	499	499	
$(^{4}A)(bpy)Co-OH^{+} + OH^{\bullet} \rightarrow (^{3}A'')16 + H_{2}O$	9	-33	9	13	-76	-72	

[&]quot;Including zero-point energy corrections. ^bFor ion structures refer to Figure 7c. ^cCalculations with the 6-311+G(2d,p) basis set. ^dCalculations with the 6-311+G(2d,p) basis set.

The 18 O labeling and action spectroscopy data pointed to the dynamical nature of the reaction of **1** with water, which was sensitive to the surrounding conditions of residual gas pressure and collisional cooling. When the reaction was performed under higher pressure conditions, the $[(bpy)Cu=O + H_2O]^+$ system followed the triplet-state trajectory forming complex **4** that was collisionally cooled and avoided crossing to the more stable singlet **6**. Under the low-pressure conditions, ca. 60% of the reacting system crossed to the singlet state. Under intermediate pressure/collision cooling conditions used in the action spectroscopy measurements, ca. 75% of the complexes remained in the triplet state.

The Ni and Co complexes showed some specific features that distinguished them from the Cu system. The doublet $(^2A'')9$ and quartet $(^4A_2)10$ states of $(bpy)Ni=O^+$ are nearly isoenergetic and each can be the reactant in the exothermic addition of water (Figure 8b, Table 2). The water adducts of the doublet-state are the nearly isoenergetic asymmetric (11) and symmetric (12) ions that can interconvert. The quartet-state products favor the asymmetric adduct 13. The more

loosely bound water in asymmetric adducts can presumably be displaced by an external water molecule to undergo exchange.

The 310 nm band in the action spectrum of the [(bpy)Ni= $O + H_2O$]⁺ ion (Figure 7a) can be fitted by the TD-DFT-calculated absorption spectra of 11 and 12 (Figure S18a, Supporting Information). However, only 11 shows bands at 340 and 400 nm to fit the action spectrum whereas the 590 nm band can originate only from 12. Hence, the action spectrum of [(bpy)Ni= $O + H_2O$]⁺ can be represented by a mixture of 11 and 12, which is also consistent with their comparable relative energies that should allow them to coexist at thermal equilibrium (Figure 8b).

The (bpy)Co=O $^+$ ions clearly favor the triplet ($^3A''$)16 state over the ($^1A'$)15 singlet (Figure 8c, Table 3). Water addition to 16 can proceed on the triplet-state potential energy surface forming exothermically the asymmetric adduct 17 that can isomerize to the final symmetric adduct (3A_2)18. The singlet potential energy surface runs parallel to and above of that of the triplet state, so no surface crossing is indicated. The final singlet-state adduct 20 is at a significantly higher energy

than 18. The action spectrum of the $[(bpy)Co=O + H_2O]^+$ ion (Figure 7b) shows a close fit with the TD-DFT-calculated absorption spectra of 17 and 18 regarding the 310 and 340 nm bands (Figure S18b, Supporting Information). The 430 nm band is represented (at 460 nm) in the calculated spectrum of 17 only. This indicates that the gas-phase ion population contains both 17 and 18. In view of its higher relative energy, the presence of complex 17 must be due to kinetic trapping. We calculated the unimolecular rate constants for the $17 \rightarrow 18$ isomerization using the RRKM theory³¹ and the ω B97X-D energies from Table 3. These indicate that 17 having 75 kJ mol⁻¹ internal energy, corresponding to 495 K rovibrational temperature, would have a 50 ms half-life which is compatible with the ion trapping time (Figure S19a,b, Supporting Information). A half-life for a fully thermalized 17 at 310 K was obtained from transition state theory as $t_{1/2} = 95$ ms (Figure S19c, Supporting Information). Hence, the presence of the higher-energy asymmetric ion 17 in the population of stable [(bpy)Co=O + H_2O]⁺ ions is not excluded by the isomerization kinetics.

Stoichiometric versus Catalytic Water Splitting. Photodissociation of the $[(bpy)M(NO_3)]^+$ ions followed by water addition and further photodissociation of the $[(bpy)M=O+H_2O]^+$ adducts achieves dissociation of the water molecule. The pertinent action spectra indicate that strong absorption bands of $[(bpy)MNO_3]^+$ and $[(bpy)M=O+H_2O]^+$ overlap at 300 nm, allowing the use of single-color photodissociation. To close the reaction cycle and achieve a catalytic photodissociation process in the gas phase, 32 the $[(bpy)M=OH]^+$ products have to be photolyzed to liberate the $[(bpy)M=O]^+$ active species. To explore this step, we obtained the action spectrum of the $[(bpy)Cu-OH]^{+\bullet}$ ion (Figure 10a) that was generated by CID of a serine ternary complex, $[(bpy)Cu(Ser-H)]^{+\bullet}$, 33 and characterized by its matching absorption spectrum from TD-

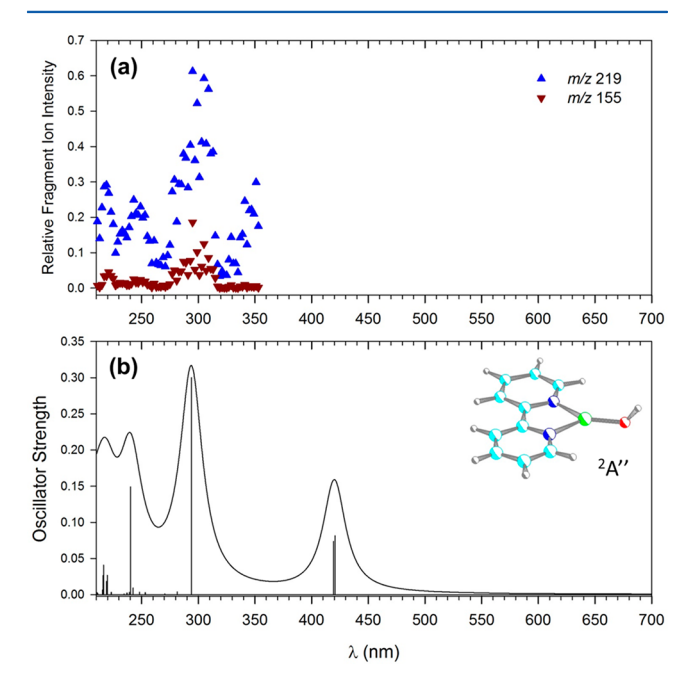


Figure 10. (a) Photodissociation action spectra of (bpy)Cu $-OH^+$ (m/z 236) (b) TD-DFT M06/6-311+G(3df,p) calculated absorption spectrum of $(^2A'')$ (bpy)Cu $-OH^{+\bullet}$ showing major transitions at 215, 240, and 294 nm. The lines were convoluted with Lorenztian functions at 12 nm full width at half-maximum.

DFT calculations (Figure 10b). The action spectrum shows a strong absorption band at 300 nm that overlaps with the absorption bands used to generate the [(bpy)Cu−OH]⁺ ion. However, photodissociation of [(bpy)Cu−OH]⁺ did not result in a loss of a hydrogen atom to reform the [(bpy)Cu= O] tions to repeat the water addition and splitting, closing the catalytic cycle.³⁴ The main dissociation channels are loss of OH and H_2O forming the m/z 219 and 218 fragment ions (Figures \$20a-c, Supporting Information). The dissociations of [(bpy)-Cu−OH]⁺ are essentially consistent with the pertinent energy thresholds (Table 1). The loss of water, forming [(bpy -H)Cu]⁺
•, has the lowest threshold energy (210 kJ mol⁻¹ relative to [(bpy)Cu−OH]⁺•) and is the dominant channel in collision-induced dissociation. The reaction is reversible, as the $[(bpy - H)Cu]^{+\bullet}$ ion adds water, and the additionelimination reactions can be cycled with trapped mass-selected ions. Loss of OH from [(bpy)Cu-OH]⁺ requires 241 kJ mol⁻¹ of threshold energy and is one of the major photodissociation channels. By contrast, loss of H from the OH group is a high-energy process of a 461 kJ mol⁻¹ threshold energy that is not triggered by even higher-energy photons (λ < 259 nm, Figure S20a). Interestingly, the O-H bond in [(bpy)Cu-OH]^{+●} is weaker than in water, as the hydrogen transfer from [(bpy)Cu−OH]⁺ to OH is calculated to be 23 kJ mol⁻¹ exothermic (Table 1). The results for the Ni and CO complexes were analogous to those for Cu in that the loss of H was energetically disfavored against the loss of OH (Tables 2 and 3).

CONCLUSIONS

Near-UV photodissociation at 300 nm can be used to drive the formation of gas-phase metal-oxo ions of the (bpy)M=O⁺ type (M = Cu, Ni, Co) that spontaneously add water in ion—molecule reactions. The resulting $[(bpy)Me=O + H_2O]^+$ complexes are photolyzed by near-UV light to eliminate OH radicals, effectively cleaving the added water molecules. The gas-phase water splitting reaction is stoichiometric, as the $[(bpy)M-OH]^+$ products do not photodissociate to reform the $(bpy)M=O^+$ reactants. The $[(bpy)M=O + H_2O]^+$ ion structures, electronic states, and dissociations were characterized by photodissociation action spectroscopy and density functional theory calculations to elucidate the processes involved in water splitting. Further efforts are needed to reform the $[(bpy)M=O]^+$ reactant ions and close the catalytic cycle.

ASSOCIATED CONTENT

S Supporting Information

The Supporting Information is available free of charge on the ACS Publications website at DOI: 10.1021/acs.jpca.7b12445.

Experimental procedures, complete reference 29, Table S1, and Figures S1–S20 (PDF)

AUTHOR INFORMATION

Corresponding Author

*E-mail: turecek@chem.washington.edu. Phone 206-685-2041. Fax: 206-685-8665.

ORCID

František Tureček: 0000-0001-7321-7858

Notes

The authors declare no competing financial interest.

ACKNOWLEDGMENTS

F.T. thanks the Chemistry Division of the National Science Foundation (Grants CHE-1661815 and CHE-1543805) for research funding, and the Klaus and Mary Ann Saegebarth Endowment for general support. Thanks are due to Jarred Olson and Professor Cody Schlenker for their help with the electrochemical synthesis of ¹⁸O labeled nitrate.

REFERENCES

- (1) http://webbook.nist.gov/chemistry/ (accessed November 22, 2017).
- (2) McEvoy, J. P.; Brudvig, G. W. Water-Splitting Chemistry of Photosystem II. Chem. Rev. 2006, 106, 4455–4483.
- (3) Joya, K. S.; Valles-Pardo, J. L.; Joya, Y. F.; Eisenmayer, T.; Thomas, B.; Buda, F.; de Groot, H. J. M. Molecular Catalytic Assemblies for Electrodriven Water Splitting. *ChemPlusChem* **2013**, 78, 35–47.
- (4) Sala, X.; Romero, I.; Rodríguez, M.; Escriche, L.; Llobet, A. Molecular Catalysts That Oxidize Water to Dioxygen. *Angew. Chem., Int. Ed.* **2009**, 48, 2842–2852.
- (5) Hurst, J. K. Chemistry in Pursuit of Water Oxidation Catalysts for Solar Fuel Production. *Science* **2010**, 328, 315–316.
- (6) Liu, X.; Wang, F. Transition Metal Complexes That Catalyze Oxygen Formation from Water:1979–2010. *Coord. Chem. Rev.* **2012**, 256, 1115–1136.
- (7) Karkas, M. D.; Verho, O.; Johnston, E. V.; Akermark, B. Artificial Photosynthesis: Molecular Systems for Catalytic Water Oxidation. *Chem. Rev.* **2014**, *114*, 11863–12001.
- (8) Tureček, F. Transient Intermediates of Chemical Reactions by Neutralization-Reionization Mass Spectrometry. *Top. Curr. Chem.* **2003**, 225, 77–129.
- (9) Schroder, D.; Holthausen, M. C.; Schwarz, H. Radical-Like Activation of Alkanes by the Ligated Copper Oxide Cation (Phenanthroline)CuO+. *J. Phys. Chem. B* **2004**, *108*, 14407–14416.
- (10) Turecek, F. Copper-Biomolecule Complexes in the Gas Phase. The Ternary Way. *Mass Spectrom. Rev.* **2007**, *26*, 563–582.
- (11) Jasikova, L.; Hanikyrova, E.; Schroder, D.; Roithova, J. Aromatic C-H Bond Activation Revealed by Infrared Multiphoton Dissociation Spectroscopy. *J. Mass Spectrom.* **2012**, *47*, 460–465.
- (12) Rijs, N. J.; Weiske, T.; Schlangen, M.; Schwarz, H. On Divorcing Isomers, Dissecting Reactivity, and Resolving Mechanisms of Propane C-H and Aryl C-X (X = halogen) Bond Activations Mediated by a Ligated Copper(III) Oxo Complex. *Chem. Phys. Lett.* **2014**, *608*, 408–424.
- (13) Yassaghi, G.; Andris, E.; Roithova, J. Reactivity of Copper(III)-Oxo Complexes in the Gas Phase. *ChemPhysChem* **2017**, *18*, 2217–2224.
- (14) Barnett, S. M.; Goldberg, K. I.; Mayer, J. M. A. Soluble Copper-Pyridine Water-Oxidation Electrocatalyst. *Nat. Chem.* **2012**, *4*, 498–502.
- (15) Kaczmarek, L.; Balicki, R.; Lipkowski, J.; Borowicz, P.; Grabowska, A. Structure and Photophysics of Deazabipyridyls. Excited Internally Hydrogen-Bonded Systems with One Proton Transfer Reaction Site. *J. Chem. Soc., Perkin Trans.* 2 **1994**, *2*, 1603–1610.
- (16) Shaffer, C. J.; Marek, A.; Pepin, R.; Slováková, K.; Tureček, F. Combining UV Photodissociation with Electron Transfer for Peptide Structure Analysis. *J. Mass Spectrom.* **2015**, *50*, 470–475.
- (17) Shaffer, C. J.; Pepin, R.; Tureček, F. Combining UV Photodissociation Action Spectroscopy with Electron Transfer Dissociation for Structure Analysis of Gas-Phase Peptide Cation-Radicals. J. Mass Spectrom. 2015, 50, 1438–1442.
- (18) Pyatkivskyy, Y.; Ryzhov, V. Coupling of Ion-Molecule Reactions with Liquid Chromatography on a Quadrupole Ion Trap Mass Spectrometer. *Rapid Commun. Mass Spectrom.* **2008**, 22, 1288–1294.
- (19) Frisch, M. J.; Trucks, G. W.; Schlegel, H. B.; Scuseria, G. E.; Robb, M. A.; Cheeseman, J. R.; Scalmani, G.; Barone, V.; Mennucci,

- B.; Petersson, G. A., et al. *Gaussian 09*, revision A.02; Gaussian, Inc.: Wallingford CT, 2009.
- (20) Becke, A. D. A. New Mixing of Hartree-Fock and Local Density-Functional Theories. *J. Chem. Phys.* **1993**, *98*, 1372–1377.
- (21) Yanai, T.; Tew, D. P.; Handy, N. C. A New Hybrid Exchange-Correlation Functional Using the Coulomb-Attenuating Method (CAM-B3LYP). *Chem. Phys. Lett.* **2004**, 393, 51–57.
- (22) Chai, J. D.; Head-Gordon, M. Long-Range Corrected Hybrid Density Functionals with Damped Atom-Atom Dispersion Corrections. *Phys. Chem. Chem. Phys.* **2008**, *10*, 6615–6620.
- (23) Zhao, Y.; Truhlar, D. G. The M06 Suite of Density Functionals for Main Group Thermochemistry, Thermochemical Kinetics, Noncovalent Interactions, Excited States, and Transition Elements: Two New Functionals and Systematic Testing of Four M06-Class Functionals and 12 Other Functionals. *Theor. Chem. Acc.* 2008, 120, 215–241.
- (24) Furche, F.; Ahlrichs, A. Adiabatic Time-Dependent Density Functional Methods for Excited State Properties. *J. Chem. Phys.* **2002**, 117, 7433–7447.
- (25) Barbatti, M.; Ruckenbauer, M.; Plasser, F.; Pittner, J.; Granucci, G.; Persico, M.; Lischka, H. Newton-X: A Surface-Hopping Program for Nonadiabatic Molecular Dynamics. Wiley Interdisciplinary Reviews: Comput. Mol. Sci. 2014, 4, 26–33.
- (26) Gatlin, C. L.; Tureček, F.; Vaisar, T. Determination of Soluble Cu(I) and Cu(II) Species in Jet Fuel by Electrospray Ionization Mass Spectrometry. *Anal. Chem.* **1994**, *66*, 3950–3958.
- (27) Osburn, S.; Ryzhov, V. Ion-Molecule Reactions: Analytical and Structural Tool. *Anal. Chem.* **2013**, *85*, 769–778.
- (28) Haddad, G. N.; Samson, J. A. R. Total Absorption and Photoionization Cross Sections of Water Vapor between 100 and 1000 A. *J. Chem. Phys.* **1986**, *84*, 6623–6626.
- (29) Garribba, E.; Micera, G.; Sanna, D.; Strinna-Erre, L. The Cu(II)-2,2'-bipyridine System Revisited. *Inorg. Chim. Acta* **2000**, 299, 253–261.
- (30) Schroder, D.; Shaik, S.; Schwarz, H. Two-State Reactivity As a New Concept in Organometallic Chemistry. *Acc. Chem. Res.* **2000**, 33, 139–145.
- (31) Gilbert, R. G.; Smith, S. C. Theory of Unimolecular and Recombination Reactions; Blackwell: Oxford, U.K., 1990; pp 52–132.
- (32) Tsybizova, A.; Roithova, J. Copper-Catalyzed Reactions: Research in the Gas Phase. *Mass Spectrom. Rev.* **2016**, 35, 85–110.
- (33) Gatlin, C. L.; Tureček, F.; Vaisar, T. Gas-Phase Complexes of Amino Acids with Copper(II) and Diimine Ligands. Part II. Amino Acids with O, N and S Functional Groups in the Side-Chain. *J. Mass Spectrom.* **1995**, *30*, 1617–1627.
- (34) Roithova, J.; Schroder, D. Selective Activation of Alkanes by Gas-Phase Metal Ions. *Chem. Rev.* **2010**, *110*, 1170–1211.